Impact-response study of lattice waves and phonons in metallic FCC nanoclusters using the Sutton-Chen potential

R.O. Ocaya[1], **J.J. Terblans**[2]

[1] Univ. of the Free State (Qwaqwa), P.Bag X13, Phuthaditjhaba 9866, RSA.
[2] Univ. of the Free State (Bloemfontein), P.O. Box 339 Bloemfontein 9300, RSA.

E-mail: ocayaro@ufs.ac.za

Abstract. We suggest a novel approach to investigate phonon propagation in an FCC lattice through bond-length oscillations in response to a single atom velocity perturbation. The lattice is modelled using the Sutton-Chen embedded atom model (EAM) without any energy loss mechanisms. We begin by showing that the concept of the cut-off distance must be abandoned to meaningfully simulate the transient behavior of nanoclusters. Oscillations are shown to arise and propagate through the lattice as a result of the interatomic potential. The waves, which have fundamental frequency and velocity, are put into the context of Debye theory and are shown to aptly postulate bulk and surface phonons. Calculations of the C_{11}, C_{12} and C_{44} directional moduli of elasticity calculated along the <100> direction on a thin, nano-sized slab-shaped Cu lattice consisting of 2281 Cu atoms are in good agreement with the literature values at the attained simulated temperature. We also show how the cluster temperature is affected by the passage of the wave.

1. Introduction

Simulation is today central to computational materials science [1, 2, 3]. It is useful to ascertain material properties that are difficult to determine experimentally [4, 5]. The simulated particle system scales range from nano to micro and beyond. Metallic nano-clusters are gaining prominence in many applications, notably in the area of fast, new electronic devices. These devices communicate using metallic interconnects on scales where quantum physics laws dominate. It is necessary to establish whether clusters can still be modelled using the traditional pairwise potentials that routinely applied to the macro-material [6, 7, 8, 9, 10, 11, 12].

In this article, we show, through simulation, that elastic oscillations arise in mechanically perturbed lattices. We then develop a phonon-method by extending these oscillations. We restrict the article to the [100] direction for illustration. Using a previously developed Sutton-Chen (SC) potential toolkit for face-centered cubic (FCC) metals [13], we simulate a system of 2281 copper particles and follow its transient and frequency responses. We then correlate the atomic displacements and velocities with the spectral densities in the material within the elastic-phonon dispersion model of Debye theory. Comparison of the results with the literature w.r.t the calculated elastic moduli and thermal properties show good agreement, indicating feasibility of the approach [14, 15].

1.1. Impulse-oscillation approach

Real lattice atoms vibrate about their equilibrium positions, with a character that depends on lattice defects [16]. An understanding of the energy states $E(\omega)$ and spectral density $g(E(\omega))$ is possible through lattice resonant frequency, ω. In this work, we suggest a *low-strain elastic* phonon method that can be simulated directly using standard MD [16]. The calculation of bulk and surface wave dispersion relies on inter-atomic elasticity, which is implicit in the pairwise potential. Figure (1) shows the simplest, homogeneous particle system. It is possible to model more advanced systems by using position and mass perturbations. Here, we consider only the unbounded, homogeneous mono-atomic, "hard-ball" atom system. Figure (2) shows the proposed harmonic mass-spring oscillator model. The initial, low-amplitude impulse is applied under the following assumptions.

(i) Energy and momentum are conserved,

(ii) The impacting atom remains uncoupled after impact,

(iii) The ensuing waves can be transverse or longitudinal.

Like other pairwise potentials, the SC potential has three regions, i.e. attractive, equilibrium, and repulsive. For Cu, it shows strong repulsion at 2.0 Å. In Figure (1), the wave $e^{i\bar{k}\cdot\bar{r}}$ of wave

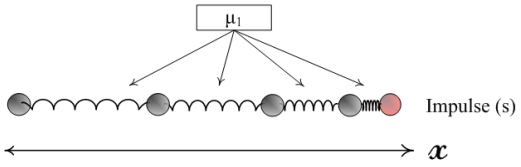

Figure 1. Mass-spring analogy of FCC structure along the x axis.

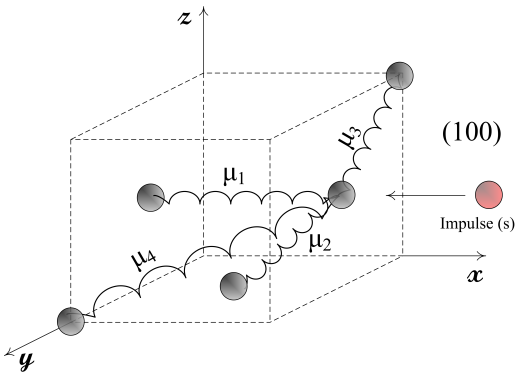

Figure 2. Homogeneous mass-spring analogy of FCC structure.

vector $\bar{k}$ at position $\bar{r}$ is clearly complex for even the simplest lattices due to the superposition from other directions. However, the simulation of such a model can describe the elastic and thermal properties of the lattice reasonably well [17, 18]. The dispersion relation for a 1-D lattice of atomic force constant μ and wave vector k is:

$$\omega^2 = (4\mu/m)\sin^2(ka/2), \tag{1}$$

where a is a lattice parameter. In the first Brillouin zone, the waves are bounded at $k{=}\pm\pi/a$ [16]. Here, we have discarded the idea of "cut-off" distance (r_{cut}), since the forces extend well beyond the boundaries of our small clusters.

2. The simulation model

The SC potential can be written as [19, 3]:

$$E_{tot} = \frac{1}{2}\sum_{ij}^{N} V(r_{ij}) + \sum_{i}^{N} F(\bar{\rho}_i), \tag{2}$$

 ISBN: 978-0-620-88875-2

where $V{=}V(r_{ij})$ is the pairwise interaction potential given by:

$$V = \varepsilon \sum_{i=1}^{N} \left(\sum_{j=i+1}^{N} \left(\frac{\sigma}{r_{ij}}\right)^{n} - c\sqrt{S_i} \right), \tag{3}$$

where

$$S_i = \sum_{j=1, j\neq i}^{N} \left(\frac{\sigma}{r_{ij}}\right)^{m}. \tag{4}$$

The term $F{=}F(\bar{\rho}_i)$ denotes the energy required to embed an atom into the array, and $\bar{r}_{ij}$ is the displacement vector between particles i and j. The force on particle i of mass m is readily shown to be

$$\overline{F}_i = -\overline{\nabla} V(r) = \varepsilon \sum_{j=1,\ j\neq i}^{N} \left[n\left(\frac{\sigma}{r_{ij}}\right)^{n} - \frac{cm}{2}\left(\frac{1}{\sqrt{S_i}} + \frac{1}{\sqrt{S_j}}\right)\left(\frac{\sigma}{r_{ij}}\right)^{m} \right] \frac{\bar{r}_{ij}}{r_{ij}^2}. \tag{5}$$

The constant ε is a dimensionless energy scaling parameter for the system, σ is the equilibrium lattice constant of the structure and c is a fitting parameter. Table 1 shows the potential and simulation parameters.

Table 1. SC and simulation parameters.

Parameter	
ε	0.012382 eV
m, n, c	6, 9, 39.432
δt	91.75 fs
t_{start}, t_{end}	0, 250 ps
T	0 K (bulk)

2.1. Simulation parameters and conditions

The thermal modelling of the system was done using energy-partitioned, independent harmonic oscillators near 0K, to limit thermal noise [20, 21]. The average atom speed v_j and temperature T are related by

$$v_j = \left(\frac{k_B T}{m}\right)^{1/2} = \left(\frac{2E_{kin}}{N_f m}\right)^{1/2}, \tag{6}$$

where E_{kin} is the total kinetic energy of all the atoms, and N_f are the available degrees of freedom. We model only irrotational translation motion, hence $N_f{=}N$. Temperatures higher than 0K but lower than melting point [20, 16] were simulated with time-step velocity equilibration [22, 23, 24, 25]. For a monoatomic lattice a density of state function, $g(\omega)$, describes available degrees of freedom up to ω_D. Its typical Debye frequencies are in the acoustic region ($\sim 10^{13}$/s) while a heterogeneous lattice has an additional branch at optical frequencies, i.e. there is now an energy band gap. We assumed an infinite lattice placed in vacuum and having no energy loss mechanism.

3. Results and Discussions

The Visual Molecular Dynamics (VMD) program [26] was used for output visualization.

3.1. Bond-length oscillations

Figures (3)-(6) show the perturbed, transient bond-length variations in the Cu lattice and their resolved discrete Fast Fourier Transforms (FFT). The equilibrium distances are 2.553 Å and 3.610 Å respectively. A comparison of the Figures (4) and (6) shows that the main peak

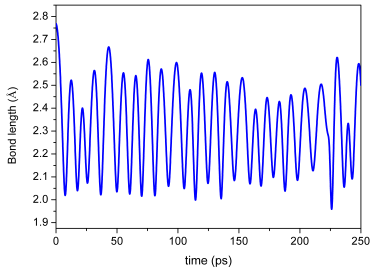

Figure 3. Amplitude transient response.

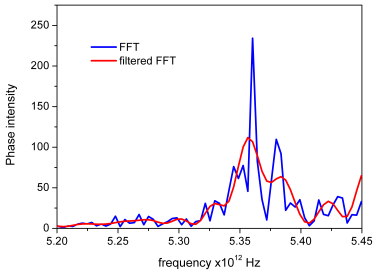

Figure 4. Phase-frequency response.

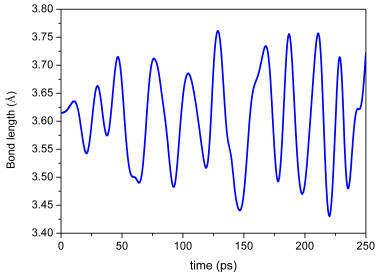

Figure 5. Amplitude transient response along [100] deep in the lattice.

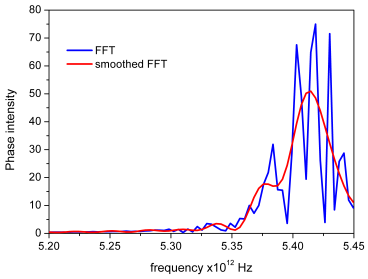

Figure 6. Phase-frequency response [100] deep in the lattice.

frequencies differ by almost 5.38 THz for two major crystal directions. The plots correspond to $\omega \approx 3.4 \times 10^{13}$/s, or phonon energy $\hbar\omega \approx 22.3$ meV, which is within the range reported empirically [27, 28]. The expected maximum vibrational frequency is $2(\mu/m)^{1/2}$ and occurs at the boundary of the first Brillouin zone [16]. We find, for Cu ($m = 63.5$ amu), that $\mu \approx 30.8$ N/m using $\omega_m \approx 3.4 \times 10^{13}$/s. The literature value is 35.32 N/m at 296K [16, 28] .

3.2. Wave propagation and the elastic constants

The moduli of elasticity $C_{\alpha\beta}$ for a cubic crystal in the Hooke's law approximation are related to the directional strain components (e_{ij}). Accepting the solution of the wave equation:

$$u(x,t) = u_0\, e^{i(kx-\omega t)}, \tag{7}$$

in terms of amplitude u_0 and wave vector $k = 2\pi/\lambda$, for the [100] direction we get

$$\omega^2\rho = C_{11}k^2 \quad \text{and} \quad \omega^2\rho = C_{44}k^2, \tag{8}$$

for a longitudinal and transverse waves, respectively.

 ISBN: 978-0-620-88875-2

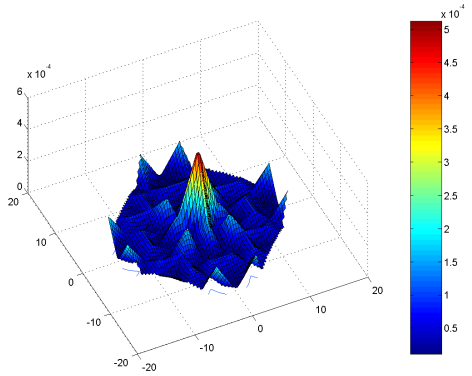

Figure 7. 3D-surface atom neighborhood.

3.2.1. Estimation of C_{11} and C_{44} Applying $\omega(k)=\omega_m$ at $k=\pi/a$ in Equation (8) gives $C_{11} = (\omega_m a/\pi)^2 \rho = (2\omega_m/\pi)^2 M/a$, with $a=b\sqrt{2}$. Using Figure (4), we get $C_{11} = 139.2 \pm 1.4$ GPa at 5.44 THz. Experimental values of 176.2 to 168.4 GPa at 0K and 300K respectively have been reported [16, 28]. The simulated diagonal bond-length (b) is 2.5487Å. The simulated bulk density of 9058 kg/m^3, as determined from $(M\sqrt{2}/b^3)$, differs from the known by less than 2%.

3.2.2. Expected temperature rise The above perturbation of the static lattice by an adatom induces propagating bulk and surface phonons [29, 30]. One therefore expects that the temperature of the overall system will increase. Figure (7), which is a 3-D thermogram of the opposite [100] face taken at the end of the simulation, shows that temperature does indeed rise.

4. Conclusions

In this article, we have suggested a standard MD method based on the Sutton-Chen embedded atom potential to simulate phonon propagation in a metallic FCC lattice. Our test bed consisted of 2281 Cu atoms. We correlated the temporal and spatial displacements with the spectral distribution. The calculated values of resonance frequencies, the elastic and other bulk constants of the lattice are in excellent agreement with empirical, literature values. Future work using the method could ascertain the effects of higher impacting energies, defects, atomic non-homogeneity and energy loss mechanisms. The method could prove valuable in the study of heat conduction of nano-clusters, with interesting implications for nano-device applications.

References

[1] Abraham MJ, Murtola T, Schulz R, Pall S, Smith JC, Hess B, Lindahl E, Gromacs: High performance molecular simulations through multi-level parallelism from laptops to supercomputers, SoftwareX 101 (2015) 88–95.
URL http://dx.doi.org/10.1016/j.softx.2015.06.001

[2] Ocaya R, Terblans JJ, Addressing the challenges of standalone multi-core simulations in molecular dynamics, in P. Ramasami (ed.), Computational Sciences, De Gruyter (2017) 1–21.
URL https://doi.org/10.1515/9783110467215-001

[3] Koleske DD, Sibener SJ, Phonons on fcc (100), (110), and (111) surfaces using Lennard-Jones potentials, Surface Science 268 (1992) 407–417.

[4] Chen ET, Barnett RN, Landman U, Crystal-melt and melt-vapor interfaces of nickel, Phys. Rev. B 40 (2) (1989) 924–932.
URL https://doi.org/10.1103/PhysRevB.40.924

[5] Chen ET, Barnett RN, Landman U, Surface melting of Ni(110), Phys. Rev. B 41 (1) (1990) 439–450.
URL https://doi.org/10.1103/PhysRevB.41.439
[6] Car R, Parrinello M, Unified approach for molecular dynamics and density functional theory, Phys. Rev. Lett. 55 (22) (1985) 2471–2474.
[7] Car R, Parrinello M, The unified approach for molecular dynamics and density functional theory, in simple molecular systems at very high density, in NATO ASI Series, Series B, Physics, P.P. Loubeyre and N. Boccara (Eds.) 186 (1989) 455–476.
[8] Remler DK, Madden PA, Molecular dynamics without effective potentials via the Car-Parrinello approach, Mol. Phys. 70 (6) (1990) 921–66.
[9] Tuckerman ME, Ab initio molecular dynamics: basic concepts, current trends and novel applications, J. Phys.: Condens. Matter.
URL stacks.iop.org/JPhysCM/14/R1297
[10] Rassoulinejad-Mousavi SM, Mao Y, Zhang Y, Physical contributions to the heat capacity of nickel, Journal of Applied Physics 119 (244304) (2016) 861–871.
URL https://doi.org/10.1063/1.4953676
[11] Chistyakova N, Tran TMH, A study of the applicability of different types of interatomic potentials to compute elastic properties of metals with molecular dynamics methods, AIP Conference Proceedings 1772 (060019) (2016) 1–7.
URL https://doi.org/10.1063/1.4964599
[12] Rushton MJD, Chroneos A, A critical assessment of interatomic potentials for ceria with application to its elastic properties revisited, Journal of Materials Science: Materials in Electronics 24 (11) (2013) 4590–4592.
URL https://link.springer.com/article/10.1007%2Fs10854-013-1447-0
[13] Ocaya R, Terblans JJ, Temperature specification in atomistic molecular dynamics and its impact on simulation efficacy, J. Phys.: Conf. Ser 905 (012031).
URL https://dx.doi.org/10.1088/1742-6596/905/1/012031
[14] Allen RE, Alldredge GP, de Wette FW, Studies of vibrational surface modes. I. General formulation, Phys. Rev. B 4 (6) (1971) 1648.
[15] Allen RE, Alldredge GP, de Wette FW, Studies of vibrational surface modes. II. Monatomic fcc crystals, Phys. Rev. B 4 (6) (1971) 1661.
[16] Kittel C, Introduction to Solid State Physics, John Wiley & Sons, New Jersey, 2005.
[17] Mohapatra M, Tolpadi S, Effects of lattice dispersion and elastic anisotropy on the thermal properties of fcc metals, Pramana 35 (2) (1990) 159–165.
[18] Meschter PJ, Wright JW, Brooks CR, Kollie TG, Physical contributions to the heat capacity of nickel, Journal of Physics and Chemistry of Solids 42 (9) (1981) 861–871.
[19] Sutton AP, Chen J, Long-range Finnis-Sinclair potentials, Philosophical Magazine 63 (1) (1990) 139–156.
[20] Schommers W, in Schommers W, von Blankenhagen P (Eds.) Structure and Dynamics of Surfaces, Springer, Berlin, 1986.
[21] Pathak LP, Rai RC, Hemkar MP, Lattice vibrations and Debye temperatures of transition metals, Journal of the Physical Society of Japan 44 (6) (1978) 1834–1838.
[22] Knuth D, The art of computer programming, seminumerical algorithms, Addison-Wesley, 1997.
[23] Box G, Muller M, A note on the operation of random normal deviates, Ann. Math Stat. 29 (1958) 610–611.
[24] Marsaglia G, The role of surface and interface structure in crystal growth, Proc. Nat. Acad. Sci. 61 (1968) 25–28.
[25] Ocaya R, Terblans JJ, Coding considerations for standalone molecular dynamics simulations of atomistic structures, J. Phys.: Conf. Ser 905 (012018).
URL https://dx.doi.org/10.1088/1742-6596/905/1/012018
[26] Theoretical and Computational Biophysics Group, Visual Molecular Dynamics, accessed: 2017-11-02.
URL http://www.ks.uiuc.edu/Research/vmd/allversions/what_is_vmd.html
[27] Ditlevsen Peter D, Nømskov Jens K, Vibrational properties of aluminum, nickel and copper surfaces, Surface Science 254 (1991) 261–274.
URL http://dx.doi.org/10.1.1.718.7356
[28] Behari J, Tripathi BB, Frequency spectra and heat capacities of copper, nickel and aluminium, Aust. J. Phys. 23 (1969) 311–318.
URL http://adsabs.harvard.edu/full/1970AuJPh..23..311B
[29] Chopra KK, Bouarab S, Off-symmetry phonon frequencies of copper, Physica status solidi (b) 125 (2) (1984) 449–504.
[30] Jani AR, Gohel VB, On the phonon frequencies of copper in off symmetry directions, Solid State Communications 41 (5) (1982) 407–411.